Available online at www.sciencedirect.com
ScienceDirect
Optics Communications 272 (2007) 107–110
OPTICS COMMUNICATIONS
www.elsevier.com/locate/optcom

Characterizing pattern dependence in transmitters and receivers for modeling optical communication systems

P. Griggio [a], J. Hu [b,*], J. Wen [b], G.E. Tudury [b,c], J. Zweck [d], B.S. Marks [b,c], L. Yan [b], G.M. Carter [b,c], C.R. Menyuk [b]

[a] *Department of Information Engineering, Università di Padova, via Gradenigo 6/A, Padova I-35131, Italy*
[b] *Department of Computer Science and Electrical Engineering, University of Maryland Baltimore County, Baltimore, MD 21250, USA*
[c] *Laboratory for Physical Sciences, College Park, MD 20740, USA*
[d] *Department of Mathematics and Statistics, University of Maryland Baltimore County, Baltimore, MD 21250, USA*

Received 18 July 2006; received in revised form 12 October 2006; accepted 21 October 2006

Abstract

We study the pattern dependences in 10 Gbit/s return-to-zero (RZ) transmitters and receivers. We describe a procedure to characterize and separate out the individual contributions from the transmitter and receiver to the pattern dependences in a 10 Gbit/s RZ system, and we validate the procedure experimentally using a transmitted pseudo-random bit string of length $2^7 - 1$.

Keywords: Optical communications; Optical receivers; Optical transmitters; Pattern dependences; *Q*-factor

1. Introduction

Accurate characterization of transmitters and receivers is necessary for the design of optical communication systems. Not only do the transmitters and receivers directly impact the system performance, but they interact with optical fiber transmission effects in a complex way. Consequently, it is not possible to accurately determine the impact of transmission effects on performance without accurate transmitter and receiver models. The importance of accurately characterizing transmitters and receivers has grown in recent years with the advent of alternatives to the traditional non-return-to-zero (NRZ) modulation format, such as the return-to-zero (RZ) and chirped-return-to-zero (CRZ) formats.

The aim of this paper is to describe a procedure to characterize and separate out individual contributions to the pattern dependence from the transmitter and receiver of a 10 Gbit/s RZ system with sufficient accuracy to allow us to reproduce the behavior in a time-domain simulation model. By pattern dependence we mean any source of waveform distortion, either optical or electrical, that causes different sequences of marks (1's) and spaces (0's) to produce a different spread of the 1-rail and the 0-rail at the decision time in the receiver in the absence of noise, and hence different *Q*-factors in the presence of noise. While the more-often-used term "intersymbol interference" is sometimes used to mean the same thing [1,2], its classical definition is far more restrictive and assumes that the detected current is the sum of currents in neighboring bits [3]. Hence, we prefer to use the term "pattern dependence."

Our goal is different from that of traditional transmitter and receiver characterization and modeling, and hence so are our methods. The traditional goal is to determine the physical effects that limit the device performance and to reduce them as much as possible [2]. Our goal is to accurately characterize the optical waveforms that emerge from the transmitter and the way in which the receiver transforms the input optical waveform prior to detection. In

* Corresponding author. Tel.: +1 410 455 6507; fax: +1 410 455 6500. *E-mail address:* hu1@umbc.edu (J. Hu).

0030-4018/$ - see front matter © 2006 Elsevier B.V. All rights reserved.
doi:10.1016/j.optcom.2006.11.026

that way, it is possible to accurately separate receiver and transmitter effects from each other and from transmission effects. The physical origin of the observed behavior, which has been the focus of traditional modeling [4–6], is of secondary importance in our paper. We have found in our own experiments that this careful separation of effects is crucial to obtain quantitatively accurate agreement between experiment and theory [7]. We have not found a careful discussion of this issue in the literature, and there are instances in the literature in which effects that are ascribed to the transmission are actually due to the transmitter and/or receiver, see e.g. [8].

A key difficulty in separately characterizing the transmitter and receiver is that they always appear together! We circumvent this difficulty by replacing the receiver with a wide-bandwidth oscilloscope at the output of the transmitter, which allows us to develop an accurate model for the transmitted signal. We note that the electrical connection to the oscilloscope introduces high-frequency oscillations, but we remove them from the time sequence, we measured at the output of the transmitter, and we do not include them in our transmitter model. We then characterize the receiver and validate the receiver model by comparing measured values of the Q-factor to those obtained by using the measured time sequence as the input noise-free signal for the receiver model and computing the resulting values of the Q-factor. Finally, to validate our transmitter and receiver model, we present results showing excellent agreement between the Q-factors obtained from simulations and experiments with a pseudo-random bit string (PRBS) of length $2^7 - 1$. As a benchmark, we also present results for the repeating 1010 pattern. Since our experimental system is a typical 10 Gbit/s RZ transmitter and receiver, we expect that the characterization procedure that we describe here will be useful in a wide range of optical communication systems.

In a back-to-back, noise-loaded experiment, the Q-factor decreases as the length of the PRBS pattern increases from $2^7 - 1$ to $2^{15} - 1$, or even longer. Such a degradation in the Q-factor can also be caused by transmission effects [9]. The first reason for focusing on strings of length $2^7 - 1$ is that the principal source of Q-factor degradation with data strings of this length is waveform distortion, whereas with longer strings the degradation also involves low-frequency effects that require a different analysis and a different approach to modeling. In particular, it is not appropriate to model long-period effects in the context of a full time-domain simulation in which the pulse shapes of the individual bits are taken into account. Thus, the work presented here serves as a necessary complement to work on longer strings. The second reason is that while strings of length $2^{15} - 1$ or even longer may represent a worst-case scenario, it is unclear that they are any more realistic in deployed systems than shorter strings. Data and voice traffic are typically digitized using line codes to avoid long, unbalanced accumulations of marks and spaces [10]. Thus, examining the behavior with shorter strings has practical importance.

2. Transmitter and receiver characterization

We performed a back-to-back experiment to investigate the impact of the bit pattern on the Q-factor. The experimental setup is shown in Fig. 1. The transmitter consisted of a CW laser at wavelength 1554.77 nm, which was modulated by a dual-stage $LiNbO_3$ modulator. The first stage of the modulator is a pulse carver used to produce 10 Gbit/s RZ pulses with a pulse duration of 44 ps, while the second stage, driven by a pulse pattern generator (PPG) and an electrical amplifier with a 3 dB bandwidth of 11 GHz, was used to encode the data at a clock rate of 9.95328 GHz. The receiver consisted of a 25 GHz optical filter, a photodiode with a 3 dB bandwidth of 20 GHz, an electrical pre-amplifier with a 3 dB bandwidth of 11.4 GHz, and a bit-error ratio (BER) tester. The optical signal is preamplified prior to receiver. To vary the optical signal-to-noise ratio (OSNR) at the receiver, we injected a variable amount of unpolarized noise from an erbium-doped fiber amplifier without any input light, while keeping the signal power fixed. We measured the OSNR with an optical spectrum analyzer (OSA) with a resolution bandwidth of 0.2 nm. We measured the BER for different values of the OSNR for both the 1010 pattern and the length $2^7 - 1$ PRBS pattern [11] and computed the Q-factor using the threshold margin method [12].

Fig. 2 shows the Q-factor as a function of the OSNR for the PRBS (squares) and 1010 (triangles) patterns. For each OSNR value, the Q-factor is smaller for the PRBS pattern than for the 1010 pattern, and the difference between the two results becomes more significant as the OSNR increases, indicating that the performance becomes more sensitive to pattern dependences. On the other hand, when the OSNR is small the performance is dominated by the optical noise [13].

We now describe a procedure to characterize the separate contributions to pattern dependent effects from the transmitter and receiver. We characterized the pattern dependences in the transmitter for the $2^7 - 1$ PRBS pattern

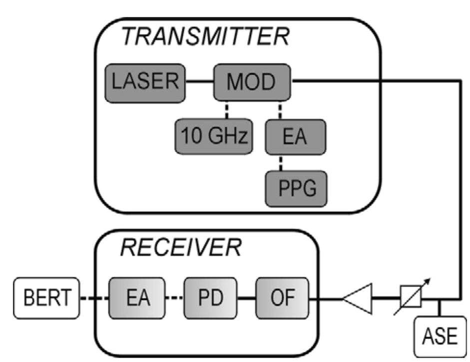

Fig. 1. Experimental setup. Solid lines correspond to optical signals and dashed lines correspond to electrical signals. OA: optical amplifier. OF: optical filter. PD: photodetector.

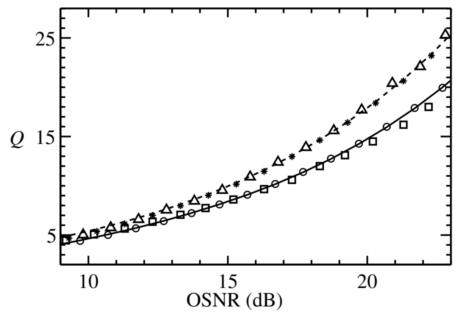

Fig. 2. The Q-factor as a function of the OSNR. The experimental data for the PRBS and 1010 patterns are shown with squares and triangles, respectively. The results obtained by combining the measured transmitter data with the receiver model are shown with circles and stars, and the simulation results with the transmitter-receiver model are shown with solid and dashed lines, respectively.

by measuring the time sequence of the optical signal immediately after the second stage of the modulator in the transmitter. This measurement was made by connecting the output optical fiber from the transmitter to a 20 GHz Agilent photodetector which was connected directly or with a short electrical cable to a 50 GHz-bandwidth oscilloscope. Simulations show that a 10 Gbit/s RZ signal is changed very little by such a wide-bandwidth photodetector and oscilloscope. In Fig. 3, we show the measured time sequence with a solid line. In a sequence of consecutive marks the peaks of the first and the last mark are usually lower than the peaks of the central marks. Similarly, the voltage of an isolated space is usually higher than that of a sequence of consecutive spaces. These observations highlight the contribution of the transmitter in decreasing the performance when transmitting a PRBS rather than a 1010 pattern. The patterning of the optical signals from the transmitter is primarily due to the patterning in the electrical signal that drives the modulator in the transmitter. Using a fast 50 GHz sampling oscilloscope, we characterized the electrical signal that drives the second stage of the modulator. The output signal of the PPG was very close to an NRZ signal with rise and fall times of about 20 ps. Similarly, we found that after the electrical amplifier the electrical signal was also well-approximated by an NRZ signal, but with rise and fall times increased to 60 ps. We attribute the increased rise and fall times to the filtering

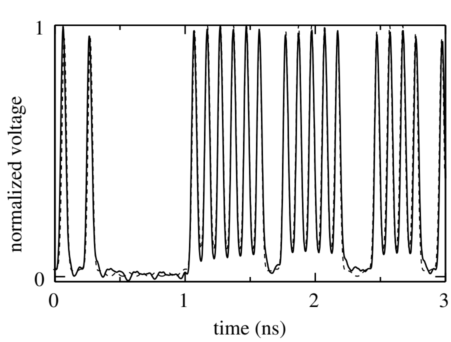

Fig. 3. The time sequence for a portion of the $2^7 - 1$ PRBS pattern. The solid and dashed lines represent the measured and simulated time sequences, respectively.

effect in the electrical amplifier, which by the convolution theorem is equivalent to a time-delayed phase and amplitude variation. Consequently, the tails of the NRZ pulses interfere with the neighboring pulses, resulting in the distortion that is visible in Fig. 3. Based on these experimental measurements, we modeled the optical signal exiting the transmitter as the product of a sequence of RZ pulses with the data-modulated NRZ signal with rise and fall times of 60 ps. We modeled the RZ pulses as Gaussian pulses with a pulse duration of 44 ps and an optical extinction ratio in the spaces of 18 dB. In Fig. 3 we compare the simulated time sequence, shown with a dashed line, to the measured time sequence. Some small, irregular oscillations are visible in the spaces of the measured time sequence. Similar oscillations were observed with the 1010 pattern. We observed that these small oscillations changed when we used different electrical cables connecting to the oscilloscope, which suggests that they are due to an electrical impedance mismatch at the oscilloscope and would not be present in the optical signal that goes to the receiver. Ignoring these small oscillations, we obtain close agreement between the simulated and measured time sequences.

Next, we characterized the contribution of pattern dependences due to the receiver. The patterning effect in the receiver also arises from waveform distortion, which we again attribute to spectral filtering to which the electrical pre-amplifier contributes most. We measured the transfer amplitude and phase functions of the pre-amplifier from 45 MHz to 40 GHz using a network analyzer. We modeled the receiver as a 25 GHz optical filter with a measured frequency response, a square-law photodiode, and an electrical filter that was modeled as the cascade of an electrical low-pass Gaussian filter with a 3 dB bandwidth of 20 GHz and the electrical pre-amplifier filter function that we derived from network analyzer measurements. To accurately compare the measured and calculated OSNR, we used the measured shape of the OSA filter in our model.

To confirm the accuracy of these experimental characterizations, we used them to compute the Q-factor using the receiver model of [14]. In this model, the Q-factor depends on the noise-free signal as a function of time just prior to the receiver, the OSNR, and the frequency response of the filters in the receiver. With these data, for each bit in the pattern, we computed the mean and standard deviation of the low-pass, electrically filtered current at the sampling time, and we then used the Gaussian approximation to the probability density function of the current in each bit to estimate the Q-factor using the decision threshold that minimizes the BER [1,14].

To validate our characterization of the receiver model, in Fig. 2 we compare the Q-factor for the PRBS pattern obtained in the experiment (squares) with that obtained using the measured time sequence as the input noise-free signal for the receiver model (circles). The excellent agreement indicates that our receiver model accurately reproduces the pattern dependences generated at the receiver. For comparison, we show the corresponding results for the 1010 pattern with triangles and stars, respectively. In both cases, we removed the irregular oscillations in the spaces that are due to impedance mismatching with the oscilloscope. Finally, in Fig. 2 we show the results with the transmitter and receiver model for the PRBS and 1010 patterns with solid and dashed lines, respectively. The agreement with the experimental results validates these models.

3. Conclusion

In this paper we have described a procedure to characterize short-length pattern dependences in a typical transmitter and receiver and to isolate their effects. We verified the correctness of this procedure in a typical 10 Gbit/s RZ transmitter and receiver with a PRBS of length $2^7 - 1$. This study may be directly applicable to line-coded data, and it provides a necessary complement to the analysis of pattern dependences due to longer bit sequences or more complicated transmitter and receiver configurations.

Acknowledgment

We would like to thank I. Lima for many useful discussions. This work was supported in part by the Nation Science Foundation.

References

[1] C.J. Anderson, J.A. Lyle, Electron. Lett. 30 (1994) 71.
[2] B.L. Kaspar, O. Mizuhara, Y.K. Chen, Optical Fiber Telecommunications, Academic Press, San Diego, CA, 2002, IV-A, p. 803 (Chapter 16).
[3] J.G. Proakis, Digital Communications, McGraw-Hill, New York, NY, 2000, p. 554 (Chapter 9).
[4] Y. Kim, S. Nam, S. Park, S. Lee, D. Jang, H.S. Kang, J. Jeong, IEEE Photon. Technol. Lett. 15 (2003) 643.
[5] D.M. Byrne, J. Lightwave Technol. 10 (1992) 1086.
[6] M. Pfennigbauer, M.M. Strasser, M. Pauer, P.J. Winzer, IEEE Photon. Technol. Lett. 14 (2002) 831.
[7] G.E. Tudury, A.S. Lenihan, G.M. Carter, in: Conference on Lasers and Electro-Optics, San Francisco, CA, 2004, Paper CTuN3.
[8] R.M. Mu, T. Yu, V.S. Grigoryan, C.R. Menyuk, J. Lightwave Technol. 20 (2002) 47.
[9] L.K. Wickham, R.J. Essiambre, A.H. Gnauck, P.J. Winzer, A.R. Chraplyvy, Photon. Technol. Lett. 16 (2004) 1591.
[10] J.C. Bellamy, Digital Telephony, Wiley, New York, NY, 2000.
[11] N.G.D. Bruijn, A combinatorial problem, in: Proceedings of the Koninklijke Nederlandse Akademie van Wetenschappen, vol. 49, 1946, p. 758.
[12] N.S. Bergano, F.W. Kerfoot, C.R. Davidson, Photon. Technol. Lett. 5 (1993) 304.
[13] J.L. Rebola, A.V.T. Cartaxo, J. Lightwave Technol. 21 (2003) 87.
[14] P.J. Winzer, M. Pfennigbauer, M.M. Strasser, W.R. Leeb, J. Lightwave Technol. 19 (2001) 1263.